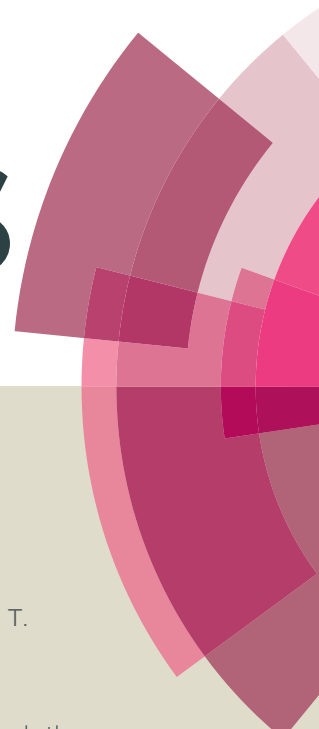


RSC Advances



This article can be cited before page numbers have been issued, to do this please use: L. Chi, J. Wang, T. Chi, Y. Qian, Z. Yu, D. Wu, Z. Zhang, Z. Jiang and J. O. Leckie, *RSC Adv.*, 2016, DOI: 10.1039/C5RA24654G.



This is an *Accepted Manuscript*, which has been through the Royal Society of Chemistry peer review process and has been accepted for publication.

Accepted Manuscripts are published online shortly after acceptance, before technical editing, formatting and proof reading. Using this free service, authors can make their results available to the community, in citable form, before we publish the edited article. This *Accepted Manuscript* will be replaced by the edited, formatted and paginated article as soon as this is available.

You can find more information about *Accepted Manuscripts* in the [Information for Authors](#).

Please note that technical editing may introduce minor changes to the text and/or graphics, which may alter content. The journal's standard [Terms & Conditions](#) and the [Ethical guidelines](#) still apply. In no event shall the Royal Society of Chemistry be held responsible for any errors or omissions in this *Accepted Manuscript* or any consequences arising from the use of any information it contains.

1 **Modeling and Optimizing Performance of PVC/PVB** 2 **Ultrafiltration Membranes Using Supervised Learning** 3 **Approaches**

4
5 Lina Chi ^{a,b,c*}, Jie Wang ^b, Tianshu Chu ^b, Yingjia Qian ^a, Zhenjiang Yu ^a, Deyi Wu ^a,
6 Zhenjia Zhang ^a, Zheng Jiang ^c, James O. Leckie ^b

7
8 ^a *School of Environmental Science and Engineering, Shanghai Jiao Tong University,*
9 *Shanghai, 200240, PRC*

10 ^b *The Center for Sustainable Development and Global Competitiveness (CSDGC),*
11 *Stanford University, Stanford, CA 94305, USA*

12 ^c *Faculty of Engineering and the Environment, University of Southampton,*
13 *Southampton, SO17 1BJ, UK*

14
15 * Correspondent author. Tel: +86 13816632156; E-mail address: lnchi@sjtu.edu.cn

16 **Abstract**

17 Mathematical models plays an important role in performance prediction and
18 optimization of ultrafiltration (UF) membranes fabricated via dry/wet phase inversion
19 in an efficient and economical manner. In this study, a systematic approach, namely, a
20 supervised, learning-based experimental data analytics framework, is developed to
21 model and optimize the flux and rejection rate of Poly (vinyl chloride) (PVC) and
22 Polyvinyl butyral (PVB) blend UF membranes. Four supervised learning (SL)
23 approaches, namely, the multiple additive regression tree (MART), the neural
24 network (NN), the linear regression (LR), and the support vector machine (SVM), are
25 employed in a rigorous fashion. The dependent variables representing membrane
26 performance response with regard to independent variables representing fabrication
27 conditions are systematically analyzed. By comparing the predicting indicators of the
28 four SL methods, the NN model is found to be superior to the other SL models with
29 training and testing R-squared values as high as 0.8897 and 0.6344, respectively, for
30 the rejection rate, and 0.9175 and 0.8093, respectively, for the flux. The optimal
31 combination of processing parameters and the most favorable flux and rejection rate
32 for PVC/PVB ultrafiltration membranes are further predicted by NN model and
33 verified by experiments. We hope the approach is able to shed light on how to
34 systematically analyzing multi-objective optimization issues for fabrication conditions
35

36 to obtain the desired ultrafiltration membrane performance based on complex
37 experiment data characteristics.

38

39 **Key words:** Poly (vinyl chloride) (PVC); Polyvinyl butyral (PVB); Supervised
40 Learning (SL) ; Neural network (NN); modeling; Membrane fabrication
41 optimization

42

43 1. Introduction

44 Poly (vinyl chloride), or PVC, is commonly used to produce relatively
45 inexpensive ultrafiltration (UF) membranes due to its relative low cost, robust
46 mechanical strength, and other favorable physical and chemical properties, such as
47 abrasive resistance, acid and alkali resistance, microbial corrosion resistance, and
48 chemical performance stability¹. Moreover, PVC membranes can usually maintain a
49 longer membrane life and remain intact after repeated cleaning with a wide variety of
50 chemical agents. However, the hydrophobic nature of PVC always leads to severe
51 fouling, thereby impeding its applications^{1,2}. Thus, a critical challenge is to improve
52 the hydrophilicity of PVC membranes without interfering with their positive
53 characteristics so that PVC-based membranes can comply with industry requirements
54 for a wider range of applications.

55 In recent years, considerable research has been conducted in order to overcome
56 this problem. Among all available methods, polymer blends often exhibit superior
57 properties when compared with a standalone, individual component polymer; in
58 addition, the polymer blend method also has the advantages of a simple procedure for
59 preparation and easy control of physical properties for various compositional changes.
60 There are several polymers that have been studied as functional polymer pairs of PVC,
61 such as PMMA¹, PU³, EVA⁴, PEO⁵, and PVB⁶ among others. In most previous
62 studies^{7,8}, PVB is found to be one of the ideal polymers to blend with PVC due to its
63 well-predicted miscible properties, chemical similarity, and less unfavorable heat
64 while mixing. In addition, owing to the –OH bond, the PVC/PVB blend demonstrates
65 more hydrophilicity than the original PVC membrane^{6,9}.

66 The selection of membrane material is essential for developing high-performance
67 membranes. However, due to the complexities of the fabrication process, even more
68 critical—especially when the membranes are made via a complex dry/wet phase

69 inversion—is a consistent and robust data analysis procedure for effectively analyzing
70 these membranes for better performance. Pure water flux (PWF) and rejection rate of
71 Bull Serum Albumin (BSA) are the most important performances for UF
72 membranes^{10,11}, depending not only upon the composition of the casting solution but
73 also upon the technical conditions used in the fabrication process. Typical variables of
74 importance for membrane development include the types and amounts of polymer,
75 additive, and the pore-forming agents used in the casting solution, the kind and
76 concentration of gelation medium, the evaporation time and temperature of the
77 spread-casting solution, the length of gelation period, and the temperature of gelation
78 bath¹² etc.. Some of the above mentioned variables have to be classified as categorical
79 variables, such as the type of the polymer, the pore-forming reagent, or the gelation
80 medium used, since they cannot be quantified. Remaining variables are quantitative
81 ones, including the temperature of evaporation or gelation, the amount of pore-
82 forming reagent added, and the duration of evaporation or gelation. Generally, these
83 complex influential factors in the membrane fabrication process would greatly delay
84 the development cycle and increase research and development (R&D) costs.
85 Therefore, it is worthwhile to investigate efficient statistical and computational
86 methods to optimize experiment design and to minimize the number of experiments.

87 Traditionally, statistically-based design of experiments (DOE) has been widely
88 used as a proper approach to optimize membrane parameters in membrane fabrication
89 processing¹³⁻¹⁵. However, DOE is based on the assumption that interactions between
90 factors are not likely to be significant^{16,17}, which is usually not the case in the real
91 world. When reducing the number of runs, a fractional factorial DOE becomes
92 insufficient to evaluate the impact of some of the factors independently¹⁶. Moreover,
93 it is also beyond the ability of DOE in dealing with categorical factors in experiments.
94 As a result, DOE has limitations in modeling a membrane fabrication process and in
95 optimizing the filtration performance of the membrane.

96 Recently, the supervised learning (SL) approach—a powerful method in
97 analyzing complex, but data-rich problems—has found strong application in diverse
98 engineering fields such as control, robotics, pattern recognition, forecasting, power
99 systems, manufacturing, optimization, and signal processing, etc.¹⁸⁻²⁰. Although the
100 idea of solving engineering problems using SL has been around for decades, it has
101 been introduced only recently into the field of material studies²¹. There are several
102 publications discussing the application of SL to the modeling and optimization of

103 membrane fabrication. S. S. Madaeni modeled and optimized PES- and PS-membrane
104 fabrication using artificial neural networks²², while Xi and Wang²³ reported that the
105 Support Vector Machine (SVM) model could be an efficient approach for optimizing
106 fabrication conditions of homemade VC-co-VAc-OH microfiltration membranes. Yet,
107 there are still a couple of key issues that need to be investigated. A systematic
108 framework for using SL approaches is required to discover the relationships between
109 membrane performance and complicated fabrication conditions.

110 The purpose of this research is to develop such a framework. More specifically,
111 we need first to evaluate experimental data quality, which is important in making
112 valid assumptions and selecting proper models for analyzing complex data. Secondly,
113 we need to develop an approach for efficiently employing reliable analysis models,
114 including the decision tree approach, neural network method, linear regression, and
115 support vector machine, for thoroughly analyzing all features and all responses of the
116 membranes, as opposed to current approaches that analyze only a single response with
117 regard to either one feature or all of the features. Finally, we need to select the most
118 suitable SL approach to predict the optimal combination of features for membrane
119 fabrication.

120

121 2. Experimental

122 2.1. Chemicals and materials

123 Unless otherwise specified, all reagents and chemicals used were of analytical
124 grade. More specifically, PVC resin ($M_w = 1.265 \times 10^5$ g/mol, and $[\eta] = 240$ mPa·s)
125 was supplied by Shanghai Chlor-Alkali Chemical Co., Ltd. $M_w = 1.265 \times 10^5$ g/mol,
126 and $[\eta] = 240$ mPa·s. PVB ($M_w = 3.026 \times 10^4$ g/mol, and $[\eta] = 40$ mPa·s) was
127 purchased from Tianjin Bingfeng Organic Chemical Co., Ltd.. N,N-
128 dimethylacetamide (DMAc) was purchased from Shanghai Lingfeng Chemical
129 Reagent Co., Ltd. PEG 600, PVP K90, and $\text{Ca}(\text{NO}_3)_2$ were purchased from Aladdin
130 Industrial Inc. BSA ($M_w = 67,000$ g/mol) was supplied by Shanghai Huamei Biological
131 Engineering Company.

132 2.2 Membrane fabrication

133 PVC/PVB composite membranes were prepared by the non-solvent induced
134 phase inversion. The casting solutions, containing PVC, PVB, DMAc, and additives,
135 were prepared in a 250 mL conical flask and heated to approximately 30-80 °C in a
136 water bath while being stirred at 600 rpm using a digital stirring machine (Fluko, GE).

137 After the polymers had been dissolved completely and stirred for at least 24 h, the
138 resulting solution was degassed for at least 30 min until no gas bubbles were visible.
139 The solution was cast on a glass plate using an 8-inch wide doctor blade with a gap of
140 200 μm between the glass plate and blade. The temperature of the blade and the glass
141 plate was controlled between 30-80 $^{\circ}\text{C}$. After a predetermined evaporation period,
142 ranging from 5 to 120 seconds, the film was immersed in a pure water or DMAc (with
143 volume concentration ranging from 10–80%) gelation bath maintained at 20 $^{\circ}\text{C}$. The
144 film was then removed from the glass plate and leached overnight in water in order to
145 completely remove any traces of solvent. Table S1 listed the various combination of
146 composition of casting solutions and corresponding processing parameters.

147 **2.3 Membrane characterization**

148 The pure water flux of the PVC/PVB blend ultrafiltration membranes was
149 measured at a temperature of 25 $^{\circ}\text{C}$ and under an operating pressure of 0.1 MPa after
150 pre-operating for 30 min. The flux of permeate was calculated according to Eq.(1):

$$151 \quad J_w = V / (A \cdot t) \quad (1)$$

152 where J_w ($\text{L}/(\text{m}^2 \cdot \text{hr})$) is the pure water flux, V (L) is the volume of the collected
153 permeate, and A (m^2) is the area of the membrane. In our study, the effective
154 membrane area is 0.0342 m^2 and t (hr) is the separation time.

155 Membrane retention ability was tested using 100 mg/L BSA at a temperature of
156 20 $^{\circ}\text{C}$ and under an operating pressure of 0.1 MPa. The concentrations of both the
157 feed water and the permeation water were determined using an ultraviolet
158 spectrophotometer (TU-1810, Beijing Purkinje Genera, China) at a wavelength of 280
159 nm. The percentage of the observed rejection solutes BSA phosphate buffer for each
160 permeate collected was calculated as the following Eq.(2):

$$161 \quad R = (1 - C_p / C_f) \times 100\% \quad (2)$$

162 where C_p is the permeate concentration and C_f is the feed concentration.

163 **3. Analyzing membrane performance by SL approaches**

164 In both this section and in Section 4, we describe a systematic framework for
165 modeling and optimizing performance of PVC/PVB ultrafiltration membranes using
166 supervised learning approaches, consisting of the following: (1) methods for
167 analyzing raw datasets and their dependencies, (2) a general procedure and algorithms
168 of SL-based data processing, (3) detailed results analysis and comparisons among all

169 SL approaches, and (4) selection of the best learning approach for optimally
170 predicting experimental performance for analyzing membrane performance.

171 **3.1 Data structures and characteristics**

172 To better understand the potential inherent structures among independent and
173 dependent variables, in this section, we first describe data structures and
174 characteristics of experimental data sets. As listed in Table S1, there are a total of 68
175 valid experimental measurements. For each measurement, we have initially identified
176 and employed 9 processing parameters that are regarded as independent variables and
177 2 performance indicators that are regarded as dependent variables. Specifically, the
178 processing parameters are PVC Wt%, DMAc Wt%, Additive Wt%, Additive type
179 (PEG600, PVPk90, Ca(NO₃)₂), Casting solution temperature (°C), Evaporation time
180 (sec), Blade temperature (°C), Gelation bath type (Water, DMAc), and Bath
181 concentration (solute concentration in gelation bath) (mg/L). Note that the types of
182 additives and the gelation bath are categorical variables. The performance indicators,
183 including the rejection rate of BSA (%) and the flux (L/(m²·h)), are numerical
184 variables. Through our preconditioning analysis, we find that the Wt% of polymers
185 and the Wt% of PVB have to be removed from the processing parameters because
186 they are dependent on, and correlated with, the change of PVC Wt%, DMAc Wt%,
187 and Additive Wt%. We introduce k as the ratio of PVC Wt%/ Polymer Wt%, giving
188 us $0 < k < 1$. There exist following relationships:

$$189 \quad \text{PVC Wt\%/k=Polymer Wt\%} \quad (3)$$

$$190 \quad \text{DMAc wt\%+Polymer Wt\%+Additive Wt\%=100\%} \quad (4)$$

191 Before the data analysis process, we briefly verify the characteristics of the data
192 by scattering the measurement points under different parameter-indicator pairs in Fig.
193 1. If the processing parameters are categorical, box-plots are used instead of scatter
194 plots. Obviously, the rejection rate and the flux are negatively correlated. For
195 numerical parameters, PVC Wt% and DMAc Wt% have the strongest correlations
196 with flux and rejection rate, respectively, while evaporation time and blade
197 temperature have cross-like scatterings, thus indicating very weak correlations. Both
198 categorical parameters can provide considerable information for performance
199 prediction. This is especially true for the additive type, where the significant
200 differences of indicators are shown between different groups of additives. In general,
201 useful information can be found in the data for performance prediction, but there are
202 not enough measurements to estimate how the indicators are distributed with regard to

203 processing parameters. In other words, our predicted indicators using SL tools will
204 have a low bias but high variance, and we need to carefully balance the accuracy and
205 stability of modeling.

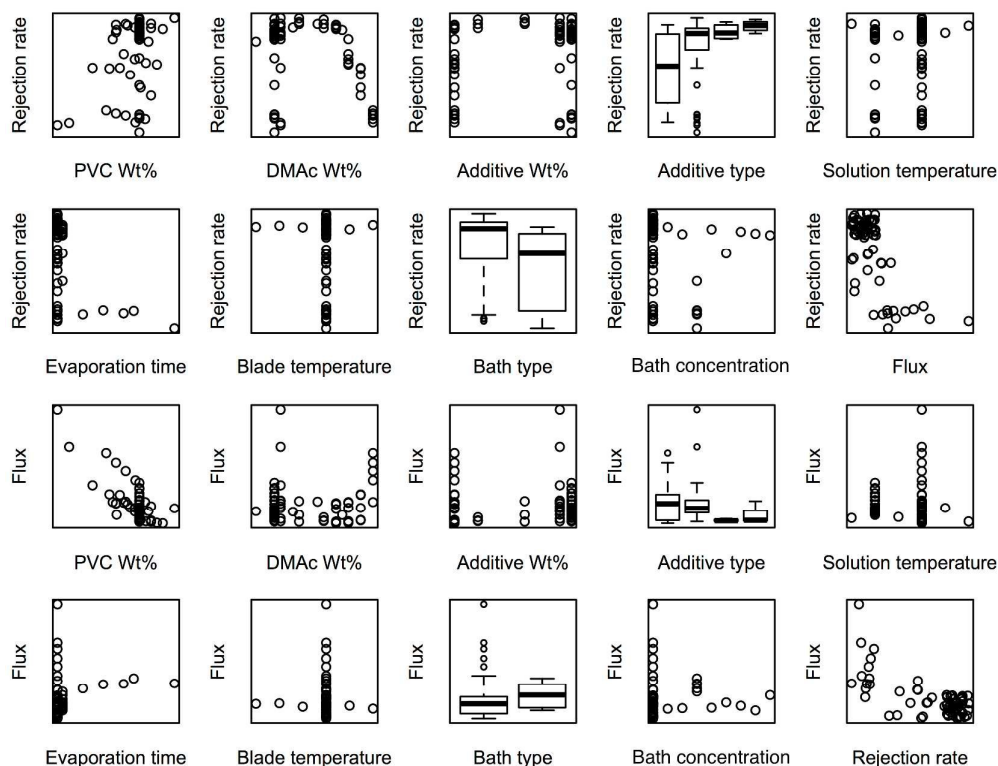


Fig. 1 Scatter plots over measurements.

206

207

208

209

3.2 Supervised learning and data analysis procedures

3.2.1 General description and criteria

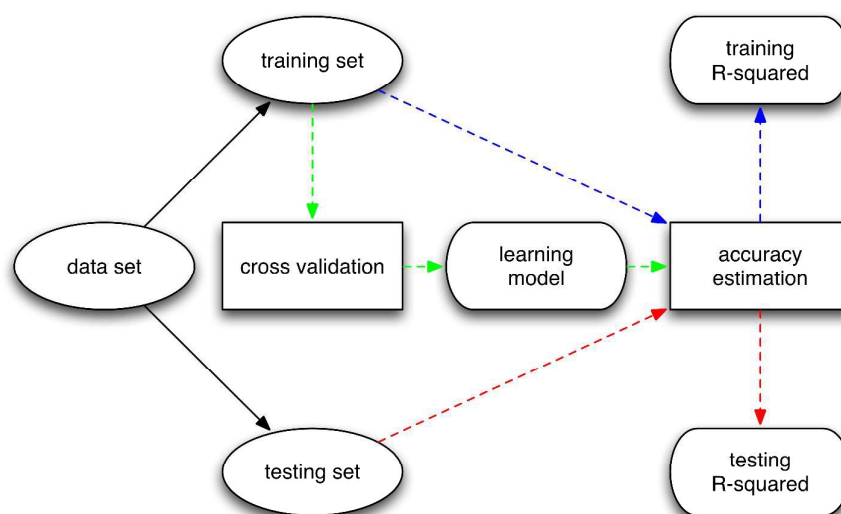
211 Different SL algorithms, including linear regression (LR), a multiple additive
212 regression tree (MART), a neural network (NN), and a support vector machine
213 (SVM), were introduced and implemented to find the potential influence of
214 processing parameters (predictors) on performance indicators (responses). The
215 advantages, limitations and assumptions when utilizing each SL algorithm were
216 described in Supporting information. To analyze the results, we train each SL
217 algorithm over the whole data.

218 Furthermore, to estimate the accuracy of each SL algorithm, we apply the Monte
219 Carlo method by repeating the learning processes 50 times on our measurement data.
220 During each learning process, we first randomly split the data into a training set and a
221 testing set, with the ratio 50/18. Next, we train each SL model based on the predictors
222 of the training set with cross-validation and make predictions of responses over the

223 training and testing sets using the trained learning model. Finally, we estimate the
224 accuracy of each model by R-squared over the training and testing sets, computed as:

$$225 \quad R^2 = 1 - \frac{\sum_{i=1}^m (\hat{y}^{(i)} - y^{(i)})^2}{\sum_{i=1}^m (\bar{y} - y^{(i)})^2} \quad (5)$$

226 where m denotes the size of the data over which we perform predictions, \hat{y} denotes
227 the prediction of each response for each array of predictors, and \bar{y} denotes the mean of
228 true responses in the data. Usually, higher training and testing R-squared values imply
229 lower bias and variance in the predictions, respectively. Fig. 2 shows the whole SL
230 process. Once we select the best SL model with the highest prediction accuracy, we
231 can train it again with all 68 data points for the further analysis.



232
233 Fig. 2 Data analysis procedure for each SL model, where ovals and rounded
234 rectangles denote the input and estimated variables, respectively

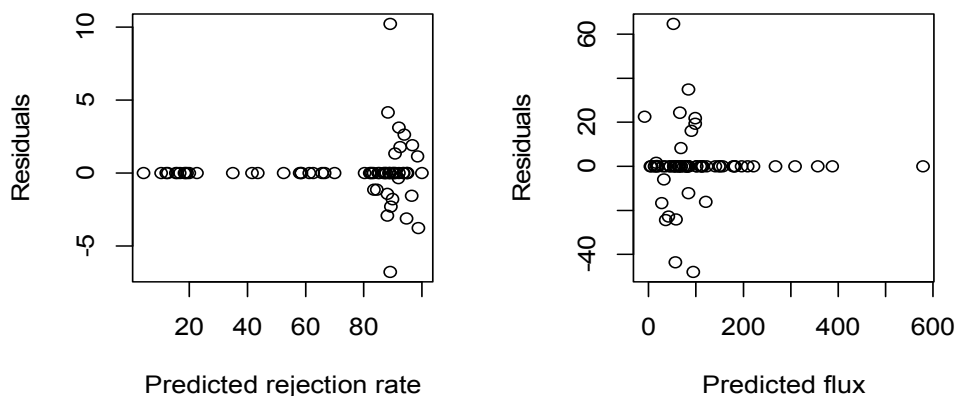
235 3.2.2 Implementation of supervised learning

236 Since our data size is small compared to the number of predictors, to avoid over-
237 fitting of NN and SVM, only statistically significant predictors are used for training.
238 Here we apply LR and MART (which are robust to irrelevant predictors) to analyze
239 and extract significant predictors. Also, cross validation is implemented to determine
240 appropriate controlling parameters of NN and SVM, for optimizing the learning
241 performance.

242 3.2.2.1 Analysis of predictors' significance

243 According to LR analysis, the coefficients of PVC Wt% and evaporation time,
244 those of DMAc Wt% and Additive Wt%, and those of additive and bath types are

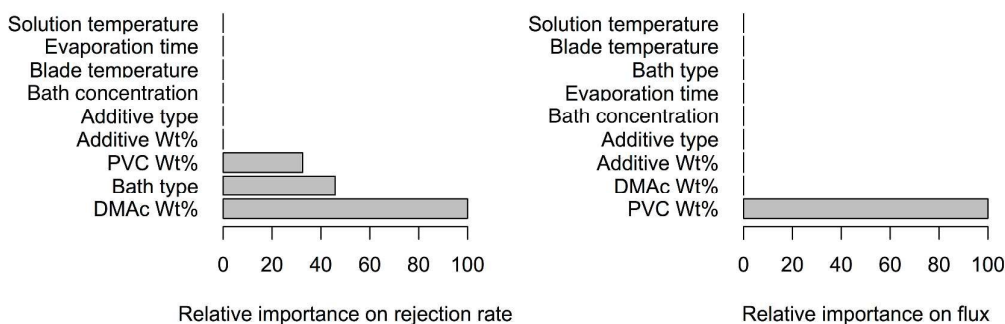
245 statistically significant at level 0, level 0.01, and level 0.05 for the rejection rate.
 246 However, there are only two statistically significant coefficients: one of PVC Wt% at
 247 level 0 and another of DMAc Wt% at level 0.1 for the flux. In other words, only a few
 248 processing parameters can provide significant information on the predictions;
 249 especially for the flux, PVC Wt% and DMAc Wt% are the two that carry the most
 250 amount of information. The low statistical significances are partially due to the small
 251 number of measurements. The linearity assumption on the relationship can be tested
 252 with R-squared values, which we will discuss later. In addition, the identical and
 253 independent distribution assumption on the noise can be tested by residual versus
 254 predicted response plots, which are shown in Fig. 3. Although the mean of residuals is
 255 indeed zero, the variance does not follow the null plot; this may be because our data is
 256 collected via a controlled parameter method.



257

258

Fig. 3 Residuals versus Predicted values plots for rejection rate and flux



259

260

Fig. 4 Importance plots of predictors on each indicator

261

262

263

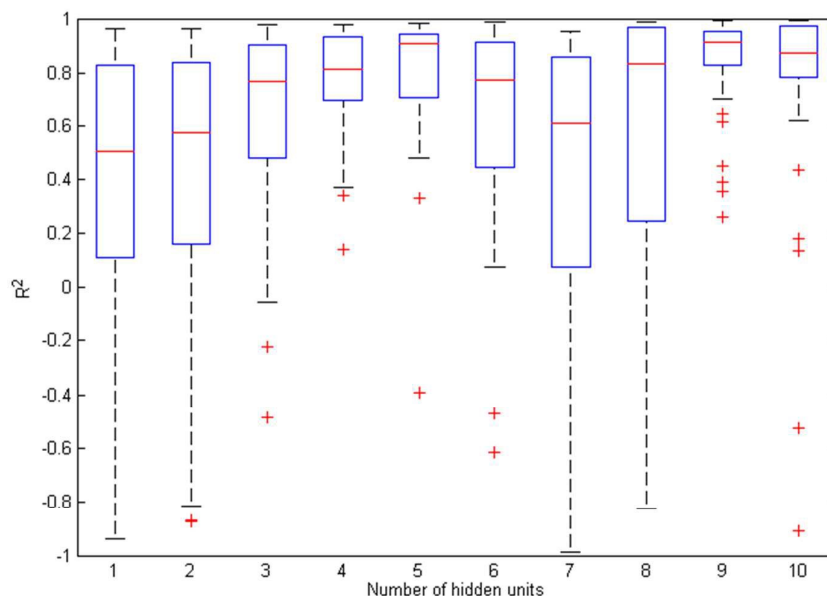
In case of MART analysis, the resulting importance rankings of each predictor for predictions are shown in Fig. 4. We can see that the number of significant predictors is even fewer than that in LR for each indicator. The importance order is

264 DMAc Wt% > Bath type > PVC Wt% for rejection rate, and only PVC Wt%
265 determines the regression tree for flux.

266 In summary, LR suggests that PVC Wt% and DMAc Wt% are the two most
267 significant predictors. MART claims that the importance order of predictors is DMAc
268 Wt% > Bath type > PVC Wt% for rejection rate, while only PVC Wt% determines the
269 regression tree for flux. Based on the results of LR and MART, we remove the
270 insignificant predictors (solution temperature) and then train NN and SVM with the
271 appropriate controlling parameters determined by cross validation.

272 3.2.2.2 Selection of appropriate controlling parameters for NN and SVM

273 As shown in Fig.1, the responses in our data are correlated, so NN is more
274 appropriate than any other SL model, which can only predict the rejection rate and the
275 flux separately. To apply NN, we should first assume that the categorical predictors
276 (additive type and bath type) are numerical. In addition, we remove the unimportant
277 predictor (solution temperature) and normalize all input predictors to zero-mean and
278 one-standard-deviation.



279
280 Fig. 5 Box-plots of testing R-squared values over 50 training processes with different
281 hidden layer sizes

282 Furthermore, we select appropriate controlling parameters. Usually, one hidden layer
283 is sufficient for a small training set. To select the optimal number of hidden units, we
284 repeat the learning processes 50 times for each, and then select the one with a high
285 mean and a low variance of testing R-squared values. During each process, we
286 randomly split the data into a training set, a validation set, and a testing set, with the

287 ratio 51/10/7, and then select the best number of epochs through cross-validation. The
288 resulting box-plots are shown in Fig. 5. We can see the optimal number of hidden
289 units is 9, with both the highest mean (0.8218) and the lowest variance of testing R-
290 squared values.

291 As regard to SVM, since our data size is small, we select only the statistically
292 significant 6 predictors in LR and MART to avoid overfitting. Furthermore, we
293 choose the appropriate controlling parameters with five-fold cross-validation. The
294 resulting support vectors are from all measurements except the 43rd or 18th
295 measurements for the rejection rate or the flux, implying the risk of over-fitting.

296

297 4. Results and discussion

298 4.1 Performance of SL models and selections

299 The training and testing R-squared values of all SL models introduced above are
300 listed in Table 1, where Rm and Rn denote the training and testing R-squared values,
301 respectively, and y1 and y2 denote the rejection rate and the flux. We can see NN is
302 the best SL model, with the highest Rm and Rn for both y1 and y2. The second best
303 SL model is SVM, which performs considerably worse for y2 and Rn.

304

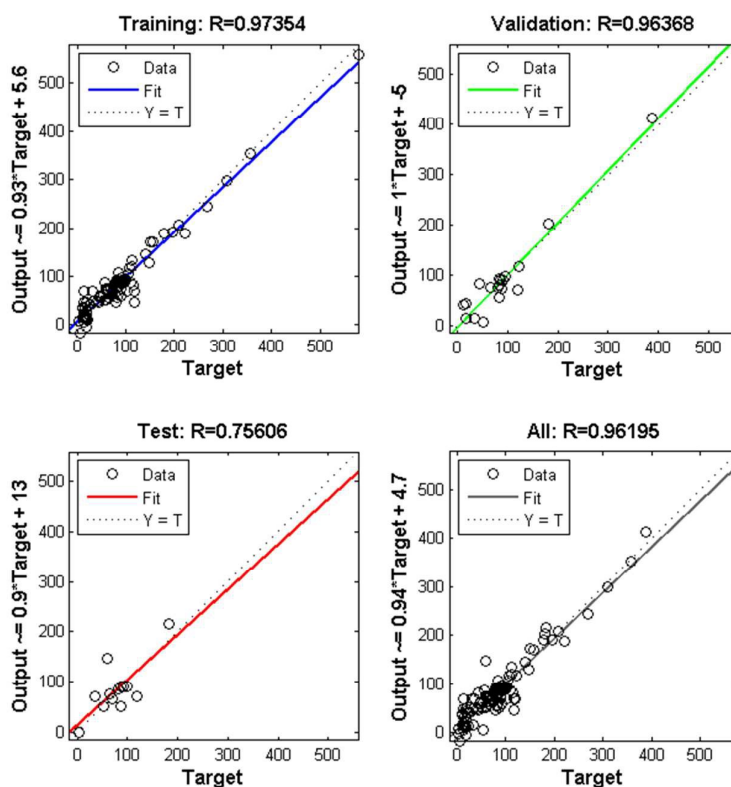
Table 1 Summary of performance of different SL models

	MART	NN	LR	SVM
Rm(y1)	0.2122	0.8897	0.6577	0.8065
Rm(y2)	0.0725	0.9175	0.6887	0.6583
Rn(y1)	0.0784	0.6344	0.3104	0.4344
Rn(y2)	-0.0329	0.8093	0.1800	0.6583

305

306 By combining the performance results in Table 1 and the properties of each SL
307 model, we can reveal some interesting underlying characteristics of the data. We
308 begin with the worst SL model, MART, which has very low R-squared values for all
309 conditions. In other words, the piecewise constant approximation does not work on
310 this data, partially due to the small number of controlled measurements. However, we
311 find that both the bias and variance are lower for the rejection rate. Thus, compared to
312 the flux, the rejection rate has relatively high order interactions with processing
313 parameters. This argument can be verified with the performance of LR. Both training
314 R-squared values are relatively high. Especially for the flux, this value is even higher

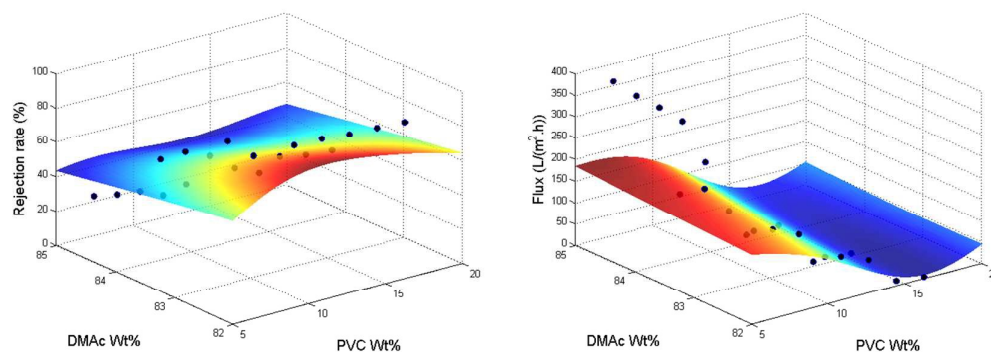
315 than that of SVM. Furthermore, SVM has much higher training R-squared of the
 316 rejection rate, and testing R-squared of both rejection and flux than those of LR.
 317 Therefore, the relationship between the flux and the processing parameters is
 318 approximately linear, but the rejection rate may have more complex and higher order
 319 interactions between the processing parameters. In addition, the noise of the
 320 measurement data is relatively high. Finally, although the testing R-squared values of
 321 SVM are much higher than LR due to the noise reduction in the higher dimensional
 322 feature space, they are still much lower than those of NN. This verifies the overfitting
 323 of SVM on small data, even when the regularization cost is set as high as 2^5 .



324
 325 Fig. 6 Prediction versus response plots for training, validation, testing, and the whole
 326 data set; target and output denote the true response and the predicted response by NN,
 327 respectively

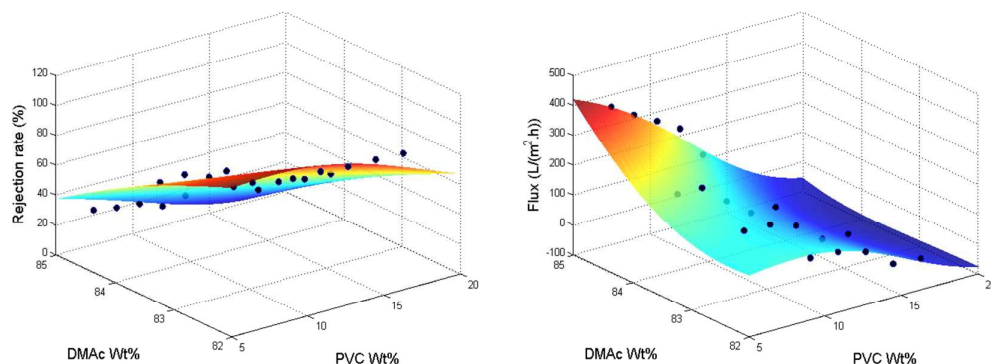
328 NN beats all other SL models in all aspects, and if the whole data is used for
 329 training, it has training R-squared values as high as 0.8992 and 0.9559 for the
 330 rejection rate and the flux. Thus, compared to the numerical approximation on
 331 categorical predictors, the correlation between the rejection rate and the flux is much
 332 more important in our predictions. To visualize the performance of NN, we plot the
 333 prediction versus the true response in Fig. 6. The performance is considered perfect if

334 the point lies on the line with intersection 0 and slope 1. Furthermore, we plot the
 335 training data points and fitting curves of SVM and NN inside the predictor subspace
 336 of PVC Wt% and DMAc Wt% in Fig. 7 and Fig. 8 by fixing all other predictors as
 337 Additive Wt% = 0%, Additive type = None, Evaporation time = 5 sec, Blade
 338 temperature = 60 °C, Bath type = Water, and volume concentration of solute in
 339 gelation bath= 0 mg/L. We can see that the fitting curves of NN are smoother and fit
 340 the training data better. In summary, because our data set is very small and noisy,
 341 the complex relationship between the rejection rate and the processing parameters is hard
 342 to fit with a good trade-off between bias and variance. Fortunately, we have the
 343 helpful information that tells us that it is correlated with the flux, which has a much
 344 simpler linear relationship, so we can apply NN to fit these two indicators.
 345



346
 347 Fig. 7 Training data and fitting curves of rejection rate and flux in the subspace of
 348 PVC Wt% and DMAc Wt% using SVM

349
 350

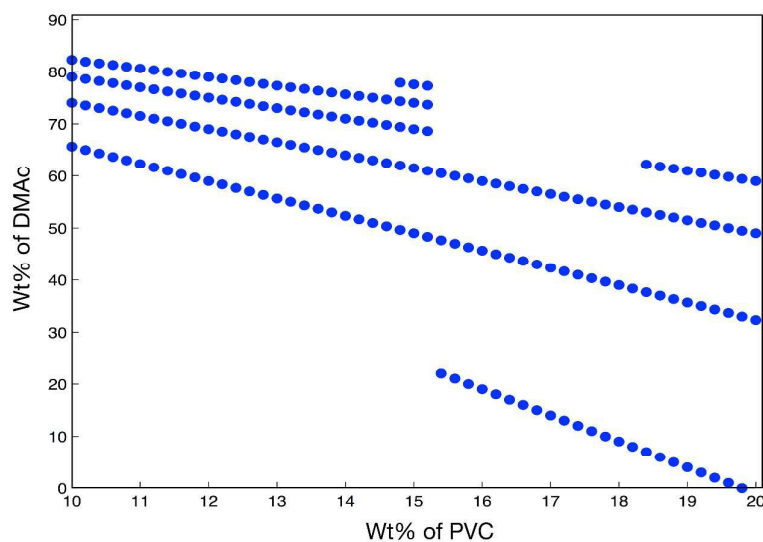


351
 352 Fig. 8 Training data and fitting curves of rejection rate and flux in the subspace of
 353 PVC Wt% and DMAc Wt% using NN

354 4.2 Optimization with NN

355 In this section, we use NN model to find the optimal combinations of processing
356 parameters to maximize the flux under the constraint that the rejection rate of BSA
357 should be no less than 80%. The idea is very simple: we search over the predictor
358 space to find certain combinations that achieve the maximum predicted flux under the
359 constraint regarding the predicted rejection rate by NN. For example, when we fix
360 Additive Wt% = 1%, Additive type = PEG600, Evaporation time = 35 sec, Blade
361 temperature = 70 °C, Bath type = Water, and Bath concentration = 0 mg/L, the
362 possible combinations of PVC Wt% and DMAc Wt% satisfying rejection rate \geq
363 80%, flux \geq 200 L/(m²·h) are scattered in Fig. 9. It is noticed that the combinations
364 are almost impossible in reality in the case of DMAc Wt% < 40% or DMAc
365 Wt% > 85%. Therefore, a question is raised here on how to perform an efficient and
366 reliable search. As a matter of fact, regarding to the problem, there exist two main
367 difficulties: (1) when searching over a high-dimensional predictor space, the
368 computation cost is very high; and (2) the predictions have high variance since the
369 size of the training data is small. To overcome these difficulties, we first narrow down
370 the search space by utilizing additional knowledge about the experiments and
371 constraints on predictors. There are several obvious constraints, such as if Additive
372 type = None, then Additive Wt% = 0%; if Bath type = water, then Bath
373 concentration = 0 mg/L. In addition, our focus is on estimating how the addition of
374 PVB into PVC improves the performance of membranes, so we introduce k as the
375 ratio of PVC Wt% / Polymer Wt%, giving us $0 < k < 1$. Furthermore, we should keep
376 the Polymer Wt% at no greater than 21%. Note that DMAc Wt% can be easily
377 calculated using Eq.3 and Eq.4.

378 So we can use k instead of DMAc Wt%. On the other hand, although the
379 prediction accuracy is not guaranteed over the whole predictor space, both training
380 and testing R-squared are very high within the data set. This means that if the search
381 points are not too far away from the measurement points, the corresponding
382 predictions are reliable. In particular, we have the search space PVC Wt% =
383 7.5:0.5:18 (%), $k = \lfloor \text{PVC Wt\%/21} \rfloor$, 0.05:0.9, and Additive Wt% = 1:1:5 (%) if
384 Additive type is not None, Evaporation time = 5:15:110 (sec), Blade temperature =
385 30:10:80 (°C), and Bath concentration = 10:10:80 (mg/L).



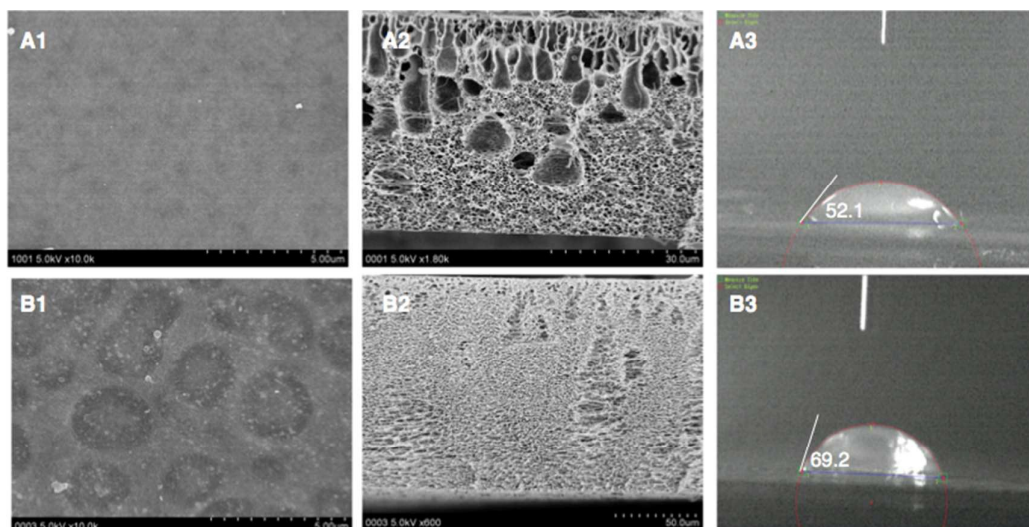
386

387 Fig. 9 Possible combinations of PVC Wt% and DMAc Wt% for specific constraints

388 on indicators fixing all other processing parameters

389 Finally, we select the combination of processing parameters that have the
 390 maximum flux under the constraint $80\% \leq \text{rejection rate} \leq 100\%$. We find with the
 391 water bath that the optimal combination of processing parameters is PVC Wt% =
 392 7.5%, DMAc Wt% = 84%, Additive Wt% = 1%, $k = 0.5$ (PVB Wt%=7.5%), Additive
 393 type = PEG600, Evaporation time = 5 (sec), and Blade temperature = 30 ($^{\circ}\text{C}$), leading
 394 to the rejection rate = 80.03% and the flux = 329.88 ($\text{L}/(\text{m}^2 \cdot \text{h})$). Similarly, in the
 395 DMAc bath, we find that when PVC Wt% = 16%, DMAc Wt% = 78%, Additive Wt%
 396 = 2%, $k = 0.8$ (PVB Wt%=4%), Additive type = PVP k90, Evaporation time = 5 (sec),
 397 Blade temperature = 30 ($^{\circ}\text{C}$), and Bath concentration= 80 (mg/L), we have the
 398 rejection rate = 81.39% and the maximum flux = 271.61 $\text{L}/(\text{m}^2 \cdot \text{h})$. Although our
 399 results are not guaranteed to be globally optimal, they are much robust than the best
 400 measurement, which has the rejection rate = 82.07% and the flux = 122.70 $\text{L}/(\text{m}^2 \cdot \text{h})$
 401 (with the processing parameters PVC Wt% = 12.6%, DMAc Wt% = 77%, Additive
 402 Wt% = 5%, $k = 0.7$ (PVB Wt%=5.4%), Additive type = PEG600, Evaporation time =
 403 10 sec, Blade temperature = 60 $^{\circ}\text{C}$, Bath type = DMAc, and Bath concentration= 80
 404 mg/L). To check the accuracy of the models used to optimize membrane performance,
 405 we fabricated PVC/PVB flat sheet membranes strictly under the above optimized
 406 parameters. Fig.10 shows the surface and cross-section morphology and the contact
 407 angle of the as-prepared membranes. In the case of pure water gelation bath, the
 408 rejection rate of the as-prepared membrane was 80.2% and the flux was 318.27

409 $L/(m^2 \cdot h)$, while in the case of DMAc as the solute of gelation bath, the as-prepared
410 membrane has the rejection rate of 86.2% and the flux of 298.5 $L/(m^2 \cdot h)$. The results
411 showed that there was a very good agreement between the model predictions and
412 experimental data.



413
414 Fig.10 Morphology and the contact angle of PVC/PVB composite membranes
415 (A: the membrane prepared under optimized parameters in the case of using pure
416 water as gelation bath, B: the membrane prepared under optimized parameters in the
417 case of using DMAc as the solute of gelation bath. 1. Surface structure 2. Cross-
418 section structure 3. Contact angle)

419 5. Conclusions

420 In this paper, we provide a systematical approach, namely, an SL-based
421 framework for experimental data analytics, for modeling and optimizing membrane
422 responses for complex combinations of membrane features during fabrication. This
423 approach consists of the following procedures. First, control experiments are
424 established to get various membranes with differing performances by combining
425 various fabrication conditions. Second, the characteristics of the feature variables are
426 analyzed in order to ascertain the quality of the data, as well as the data dependencies
427 among the variables. Third, four SL approaches (MART, NN, LR, SVM) are
428 employed to systematically analyze membrane performance and fabrication
429 conditions in a rigorous fashion. Finally, the most reliable and trustful SL model is
430 selected to optimize the fabrication conditions and predict the most favorable
431 performance of PVC/PVB ultrafiltration membranes. During this last step, we analyze
432 multiple responses simultaneously with multiple input feature variables. In this way,

433 we eliminate most unnecessary assumptions that are traditionally proposed by other
434 methods. In addition, this approach simplifies the analysis process by using a unified
435 SL framework that has been thoroughly investigated by machine learning
436 communities²⁴. This advantage surpasses previously reported DOE approaches in that
437 these standard SL approaches provide smaller biases and variances for data analysis.
438 Thus, the SL approaches offer us a more standard method not only in procedure but
439 also with more rigorous results.

440 Additionally, we glean several interesting findings from this research. One is
441 how to find the optimal mixture of feature compounds for the fabrication processes
442 more effectively and efficiently. Another is that among the tested SL approaches, the
443 NN method provides the most reliable and trusted results. In the future, we will
444 investigate how to develop a recursive and automated data-driven experimental
445 analytics approach to design performance-specific membranes more effectively and
446 efficiently.

447

448 **Acknowledgments**

449 We acknowledge financial support from the Division of International
450 Cooperation & Exchange of Shanghai Jiao Tong University, China and the Newton
451 Research Collaboration Award from Royal Academy of Engineering, UK (Reference:
452 NRCP/1415/261). In addition, we are grateful to sponsors of the Center for
453 Sustainable Development & Global Competitiveness (CSDGC) at Stanford University
454 for additional financial support. Special thanks are given to the researchers at CSDGC
455 for their technical support. Additionally, we thank Weimin Wu and Ting Wang for
456 their valuable discussion.

457

458 **References:**

- 459 1 S. Ramesh, A. H. Yahaya and A. K. Arof, *Solid State Ionics*, 2002, **148**, 483–486.
- 460 2 Z. Yu, X. Liu, F. Zhao, X. Liang and Y. Tian, *J. Appl. Polym. Sci.*, 2015, **132**,
461 41267.
- 462 3 N. Wang, A. Raza, Y. Si, J. Yu, G. Sun and B. Ding, *Journal of Colloid and*
463 *Interface Science*, 2013, **398**, 240–246.
- 464 4 S. Chuayjuljit, R. Thongraar and O. Saravari, *Journal of Reinforced Plastics and*
465 *Composites*, 2008, **27**, 431–442.
- 466 5 M. Jakic, N. S. Vrandecic and I. Klaric, *Polymer Degradation and Stability*,
467 2013, **98**, 1738–1743.
- 468 6 X. Zhao and N. Zhang, *Journal of Tianjing University of Science and*
469 *Technology*, 2007, **22**, 36–39.

- 470 7 J. zhu, L. Chi, Y. Zhang, A. Saddat and Z. Zhang, *Water Purification*
471 *Technology*, 2012, **31**, 46–54.
- 472 8 Y. Peng and Y. Sui, *Desalination*, 2006, **196**, 13–21.
- 473 9 Y. Sui, *Beijing University of Technology Thesis for Master Degree*, Beijing,
474 China, 2004, 24–26.
- 475 10 X. Zhao and K. Xu, *Plastics Sci. & Technology*, 2010, 1–6.
- 476 11 E. Corradini, A. F. Rubira and E. C. Muniz, *European polymer journal*, 1997, **33**,
477 1651–1658.
- 478 12 S.Y. L. Leung, W.H. Chan and C.H. Luk, *Chemometrics and Intelligent*
479 *Laboratory Systems*, 2000, **53**, 21–35.
- 480 13 S.Y. Lam Leung, W.H. Chan, C.H. Leung and C.H. Luk, *Chemometrics and*
481 *Intelligent Laboratory Systems*, 1998, **40**, 203–213.
- 482 14 W.H. Chan and S.C. Tsao, *Chemometrics and Intelligent Laboratory Systems*,
483 2003, **65**, 241–256.
- 484 15 M. Khayet, C. Cojocar, M. Essalhi, M. C. García-Payo, P. Arribas and L.
485 García-Fernández, *DES*, 2012, **287**, 146–158.
- 486 16 L. Wenjau and O. Soonchuan, *Computer and Automation Engineering (ICCAE),*
487 *2010 The 2nd International Conference*, 2010, **2**, 50–54.
- 488 17 P. W. Araujo and R. G. Brereton, *Trends in Analytical Chemistry*, 1996, **15**, 63–
489 70.
- 490 18 K. I. Wong, P. K. Wong, C. S. Cheung and C. M. Vong, *Energy*, 2013, **55**, 519–
491 528.
- 492 19 Y. Reich and S. V. Barai, *Artificial Intelligence in Engineering*, 1999, **13**, 257–
493 272.
- 494 20 B. L. Whitehall, S.-Y. Lu and R. E. Stepp, *Artificial Intelligence in Engineering*,
495 1990, **5**, 189–198.
- 496 21 F. J. Alexander and T. Lookman, *Novel Approaches to Statistical Learning in*
497 *Materials Science*, Informatics for Materials Science and Engineering, 2013.
- 498 22 S. S. Madaeni, N. T. Hasankiadeh, A. R. Kurdian and A. Rahimpour, *Separation*
499 *and Purification Technology*, 2010, **76**, 33–43.
- 500 23 X. Xi, Z. Wang, J. Zhang, Y. Zhou, N. Chen, L. Shi, D. Wenyue, L. Cheng and
501 W. Yang, *DESALINATION AND WATER TREATMENT*, 2013, **51**, 3970–3978.
- 502 24 C. M. Bishop, *Pattern Recognition and Machine Learning*, Springer Verlag,
503 2006.
- 504

Figures

Fig. 1 Scatter plots over measurements

Fig. 2 Data mining procedure for each SL model, where ovals and rounded rectangles denote the input and estimated variables, respectively

Fig. 3 Residuals versus Predicted values plots for rejection rate and flux

Fig. 4 Importance plots of predictors on each indicator

Fig. 5 Box-plots of testing R-squared values over 50 training processes with different hidden layer sizes

Fig. 6 Prediction versus response plots for training, validation, testing, and the whole data set; target and output denote the true response and the predicted response by NN, respectively

Fig. 7 Training data and fitting curves of rejection rate and flux in the subspace of PVC Wt% and DMAc Wt% using SVM

Fig. 8 Training data and fitting curves of rejection rate and flux in the subspace of PVC Wt% and DMAc Wt% using NN

Fig. 9 Feasible combinations of PVC Wt% and DMAc Wt% for specific constraints on indicators fixing all other processing parameters

Fig. 10 Morphology and the contact angle of the as-prepared optimized membranes (A: the membrane prepared under optimized parameters in the case of using pure water as gelation bath, B: the membrane prepared under optimized parameters in the case of using DMAc as the solute of gelation bath. 1. Surface structure, 2. Cross-section structure, 3. Contact angle.)

Figure 1

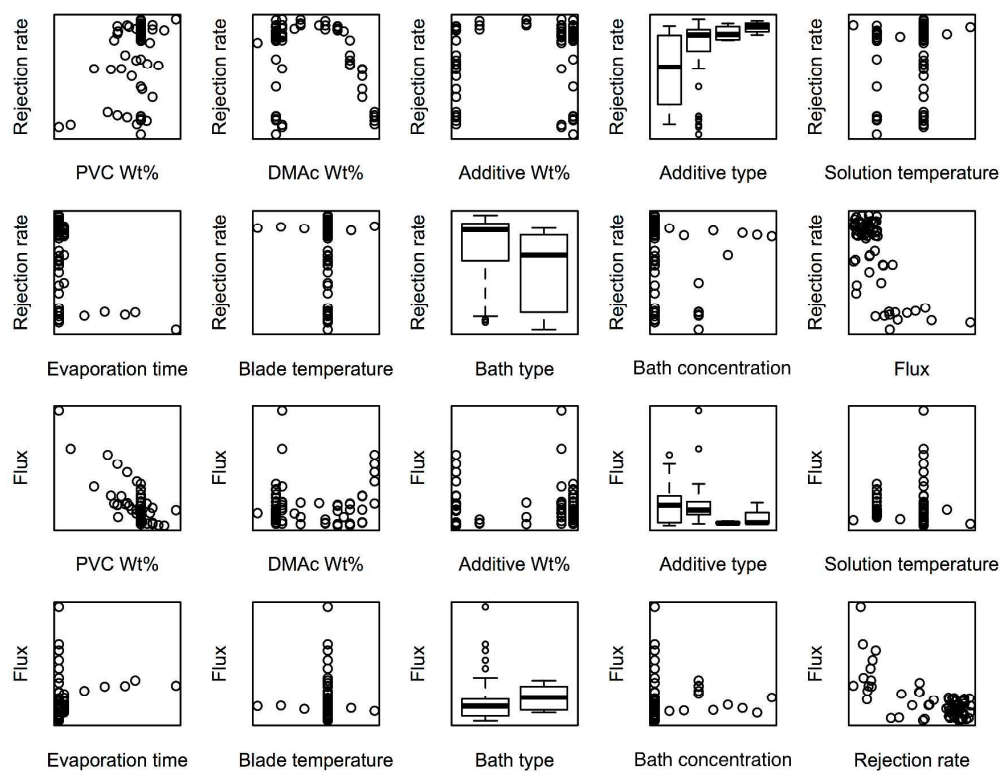


Figure 2

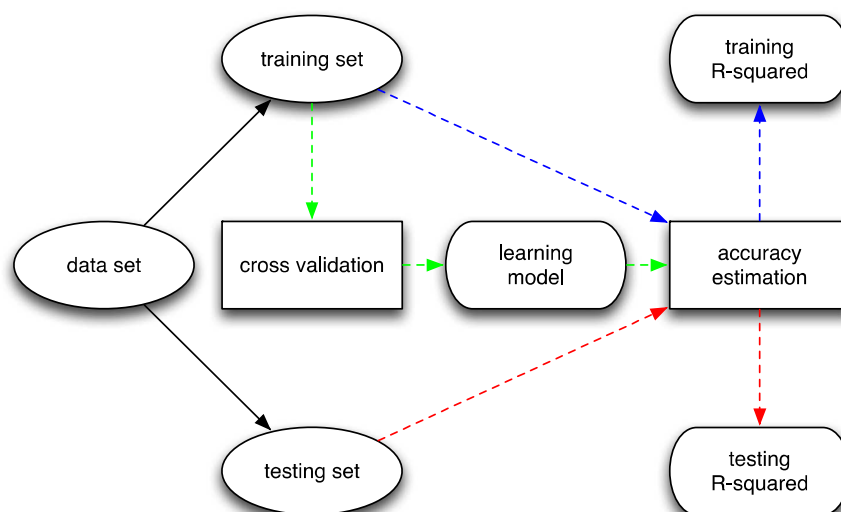


Figure 3

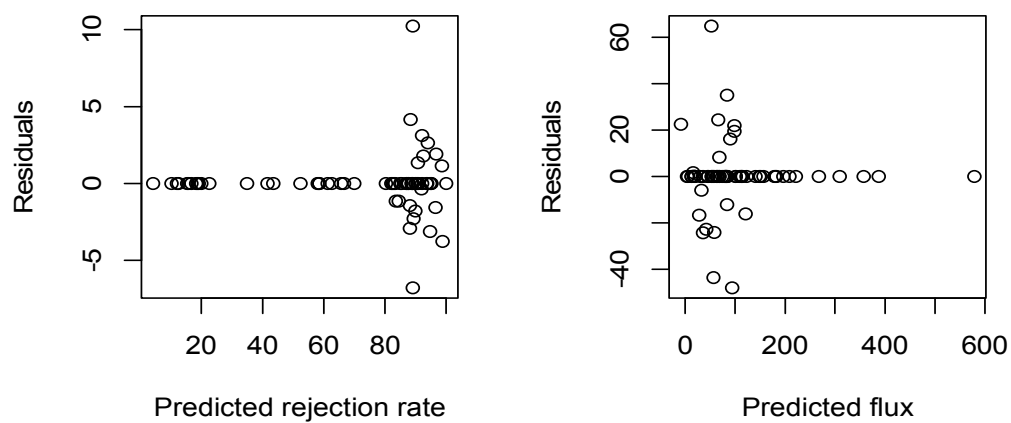


Figure 4

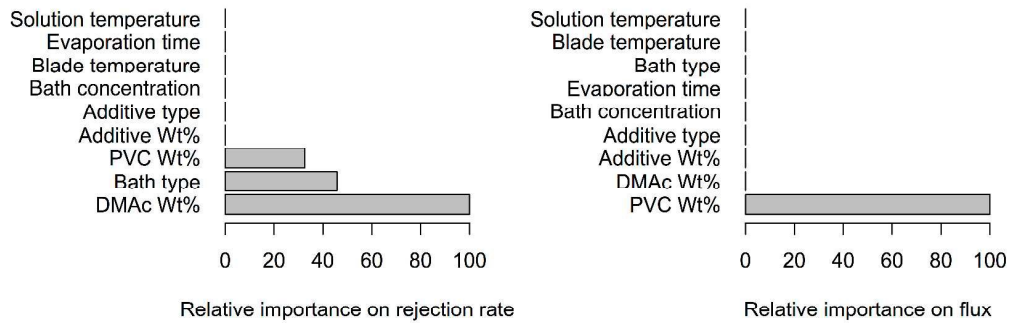


Figure 5

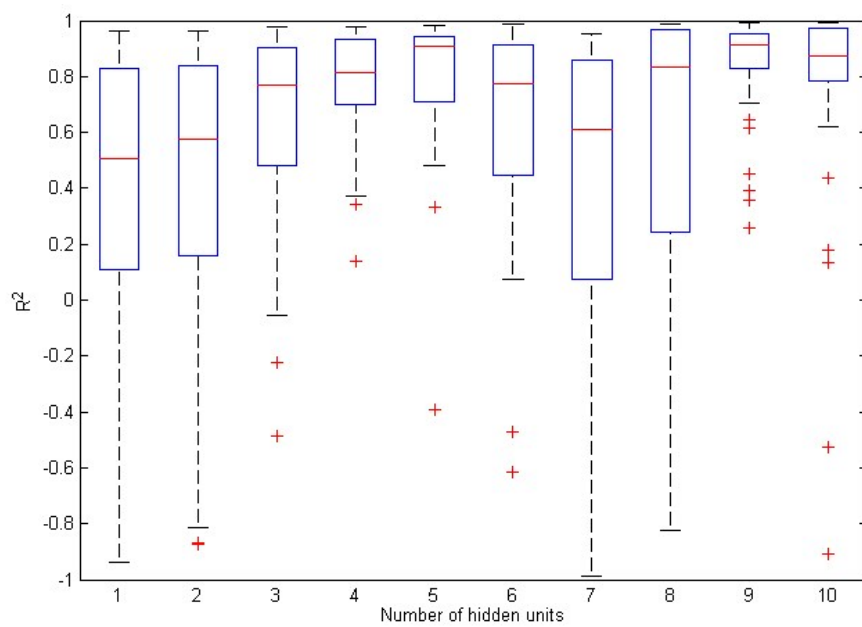


Figure 6

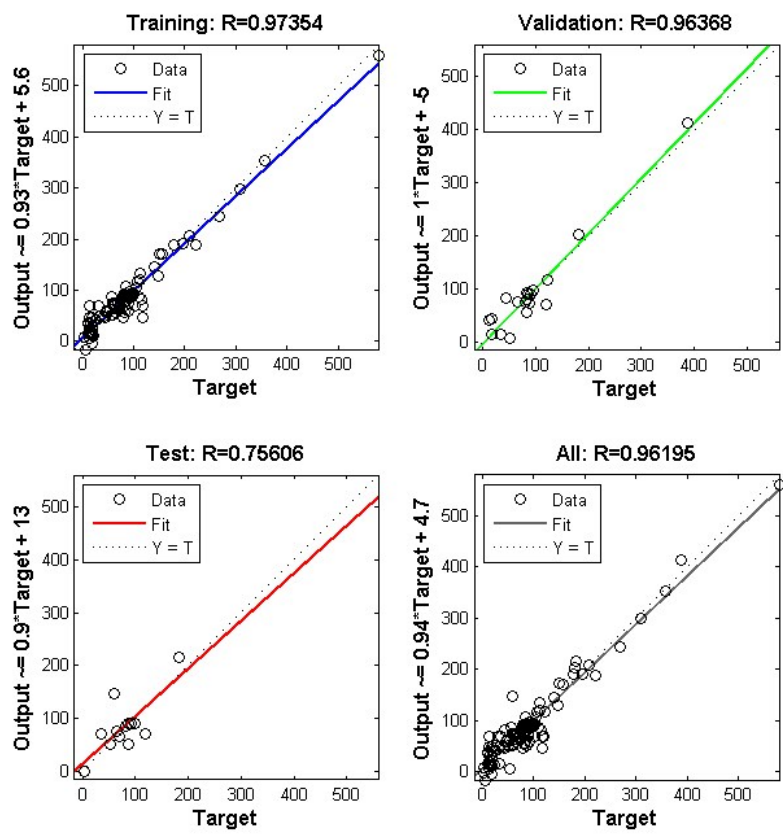


Figure 7

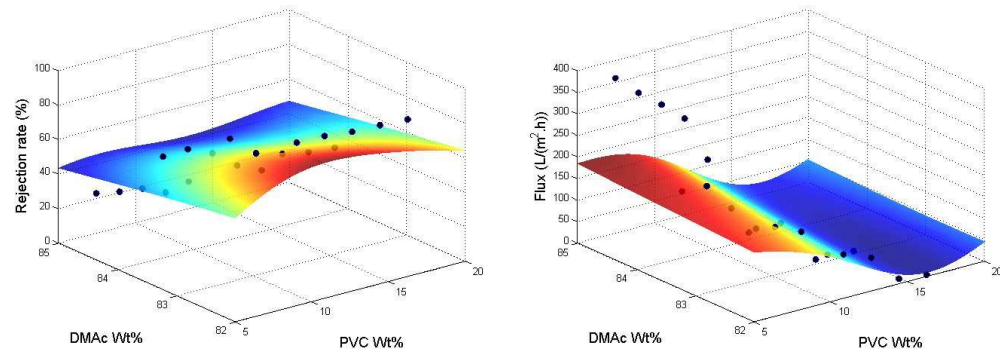


Figure 8

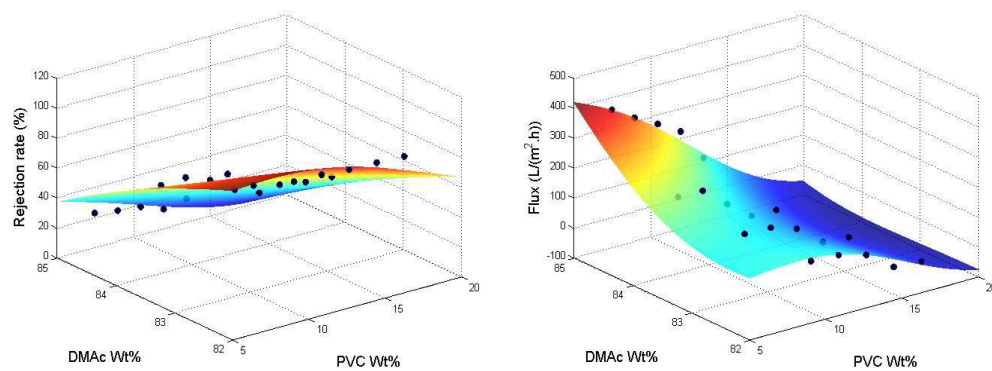


Figure 9

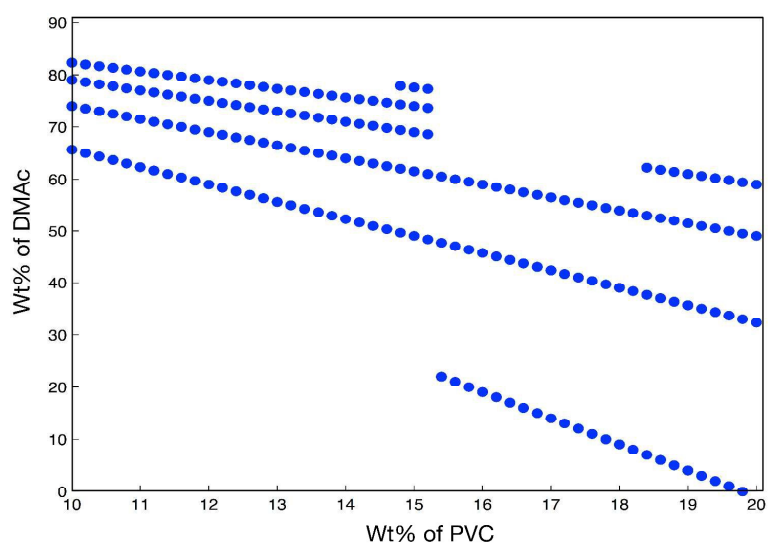
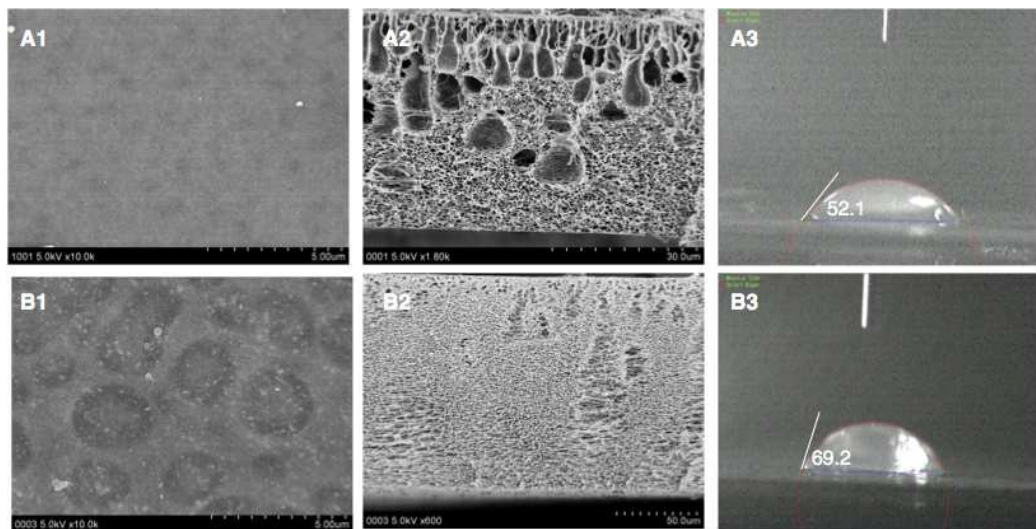


Fig. 10



Tables

Table.1 Summary of performance of different SL models

Table 1

	MART	NN	LR	SVM
Rm(y1)	0.2122	0.8897	0.6577	0.8065
Rm(y2)	0.0725	0.9175	0.6887	0.6583
Rn(y1)	0.0784	0.6344	0.3104	0.4344
Rn(y2)	-0.0329	0.8093	0.1800	0.6583

Graphical abstract

